International Journal of Electrical, Electronic and Communication Sciences
ISSN: 2517-9438
Vol:8, No:12, 2014

Grid-Connected Inverter Experimental Simulation and Droop Control Implementation

Nur Aisyah Jalalludin, Arwindra Rizqiawan, Goro Fujita

***Abstract*—**In this study, we aim to demonstrate a microgrid system experimental simulation for an easy understanding of a large-scale microgrid system. This model is required for industrial training and learning environments. However, in order to create an exact representation of a microgrid system, the laboratory-scale system must fulfill the requirements of a grid-connected inverter, in which power values are assigned to the system to cope with the intermittent output from renewable energy sources. Aside from that, during fluctuations in load capacity, the grid-connected system must be able to supply power from the utility grid side and microgrid side in a balanced manner. Therefore, droop control is installed in the inverter's control board to maintain a balanced power sharing in both sides. This power control in a stand-alone condition and droop control in a grid-connected condition must be implemented in order to maintain a stabilized system. Based on the experimental results, power control and droop control can both be applied in the system by comparing the experimental and reference values.

***Keywords*—**Droop control, droop characteristic, grid-connected inverter, microgrid, power control.

I. Introduction

IN recent years, production of greenhouse gases from fossil fuel combustion contributes to increment in global temperature and causing various impacts to human and environment. Apart from that, increasing demand in energy can cause problems such as grid imbalance [1] and thus, more power plants need to be built. Therefore, in generating new sources of energy, implementation of renewable energy such as solar energy and wind energy should be maximized. In order to create a clean energy generation system, the system cannot depend entirely to the renewable energy sources as intermittent output from the sources will affect the stability of the system. Thus, a small-scale power generation and distribution system known as microgrid was created and connected to the main grid while maintaining a synchronized frequency and voltage levels.

Microgrids are located at distribution levels and have at least one dispersed energy generation (DG) sources such as wind turbine, photovoltaic cells, or storage devices forming interconnection with the utility power generation with minimal disturbances while supplying energy to local loads. [2] Microgrids can also be operated in islanding mode when grid disturbances occur at the existing power utility to prevent wide-scale power outages. Several microgrid research projects have been developed in recent years such as Consortium for Electric Reliability Technology Solutions (CERTS) MicroGrid [3] and European Union (EU) Microgrids Research Project. [4]

In order to achieve a flexible operation between grid-forming mode and grid-injecting mode in a microgrid system, a control design with adaptive droop regulation method was proposed by J. C. Vasquez et al. [5] in which voltage and current is examined at the point of common coupling to modify the droop parameters. Droop control refers to an equal sharing of load between generating units operating in parallel [6], for instance, dispersed energy generation system. Each generating units has its own droop characteristic that determines the power output from each unit according to load changes and enables load sharing simultaneously.

In this research, a laboratory scale of microgrid system was introduced and islanding-mode operation experiments are conducted prior to grid-connected mode experiment. The main objective of this research is to develop a balanced microgrid system experimental simulation for learning environments as well as industrial training, and implementing droop control in the system. The load capacity was changed while maintaining a constant frequency level without exceeding nominal value. Inverter is the most vital part of this research as it operates to monitor the voltage and current values at both grid side and microgrid side while controlling the power supplied from the microgrid side by comparing to the power levels in the grid side.

II. Grid-Connected Inverter

Grid-connected inverter is an inverter which is connected directly to the electric grid including transmission grid and distribution grid. It converts DC output from renewable energy generation such as photovoltaic cells and small hydroelectric generation into AC output. A balanced frequency and voltage levels synchronized with the grid is the most important factor to make an interconnection between the inverter and the grid. In order to satisfy both grid-forming connection and grid-connected condition, the inverter is controlled by assigning values of several parameters such as frequency, voltage, and power at the point of common coupling (PCC) to its control system.

These parameters are vital for the safety of both microgrid and the power utility. For example, during faults at the power utility side, connection with inverter will be stopped and the inverter will operate in islanding mode. In this mode of operation, power will only be supplied by dispersed energy

N. A. Jalalludin is with the Graduate School of Electrical Engineering and Computer Science, Shibaura Institute of Technology, Tokyo 135-8548 Japan (phone: +818044722507; e-mail: ma13065@shibaura-it.ac.jp).

A. Rizqiawan is with the School of Electrical Engineering and Informatics, Institute of Technology Bandung, Jawa Barat 40116, Indonesia (e-mail: windra@stei.itb.ac.id).

G. Fujita is with the Electrical Engineering Department, Shibaura Institute of Technology, Tokyo 135-8548 Japan (e-mail: gfujita@sic.shibaura-it.ac.jp).

generation in the microgrid. During grid-connected mode, power will be supplied from both microgrid and electrical grid. Power generation in microgrid side can also provide power flow to the utility during power shortage. Thus, a grid-connected inverter was connected to a control system that drives the switching process of the inverter by using Pulse-Width Modulation (PWM).

A simple structure of the grid-connected inverter connection used in this study is shown in Fig. 1. The inverter was connected to the electric grid through an inductance, L which represents transmission lines. During islanding mode, constant voltage and frequency output was produced by grid-connected inverter to be supplied to local loads in a microgrid. In order to make a connection to the grid, the output from inverter must be in range with the power and frequency values at PCC. Once this condition is met, the synchronization process can be performed. Control of the inverter was performed by using C-language software codes converted to binary file downloaded into Digital Signal Processor (DSP) chip in the control board. The software codes include processing blocks that are required to construct the control system of the inverter.

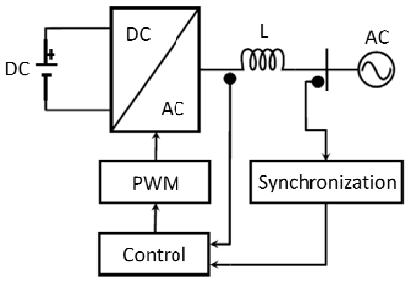

Fig. 1 Grid-connected inverter connection structure

III. Grid-forming Mode Control

A. Clarke Transformation

Clarke transformation, also known as αβ0 transformation converts three-phase instantaneous voltages, v_a v_b and v_c into two-phase stationary reference frame denoted as α and β. Transformation of the instantaneous two-phase voltage reference, v_α , v_β and a third variable known as the zero-sequence component, v_0 is shown in (1). The inverse transformation of (1) is expressed in (2).

$$\begin{bmatrix} v_\alpha \\ v_\beta \\ v_0 \end{bmatrix} = \sqrt{\frac{2}{3}} \begin{bmatrix} 1 & -\frac{1}{2} & -\frac{1}{2} \\ 0 & \frac{\sqrt{3}}{2} & -\frac{\sqrt{3}}{2} \\ \frac{1}{\sqrt{2}} & \frac{1}{\sqrt{2}} & \frac{1}{\sqrt{2}} \end{bmatrix} \begin{bmatrix} v_a \\ v_b \\ v_c \end{bmatrix} \quad (1)$$

$$\begin{bmatrix} v_a \\ v_b \\ v_c \end{bmatrix} = \sqrt{\frac{2}{3}} \begin{bmatrix} 1 & 1 & \frac{1}{\sqrt{2}} \\ -\frac{1}{2} & \frac{\sqrt{3}}{2} & \frac{1}{\sqrt{2}} \\ -\frac{1}{2} & -\frac{\sqrt{3}}{2} & \frac{1}{\sqrt{2}} \end{bmatrix} \begin{bmatrix} v_\alpha \\ v_\beta \\ v_0 \end{bmatrix} \quad (2)$$

Zero-sequence voltage, v_0 is eliminated when the three-phase voltage in a four-wire system is in a balanced condition [7] and thus simplifying (1) into a more simplified equation, (3):

$$\begin{bmatrix} v_\alpha \\ v_\beta \end{bmatrix} = \sqrt{\frac{2}{3}} \begin{bmatrix} 1 & -\frac{1}{2} & -\frac{1}{2} \\ 0 & \frac{\sqrt{3}}{2} & -\frac{\sqrt{3}}{2} \end{bmatrix} \begin{bmatrix} v_a \\ v_b \\ v_c \end{bmatrix} \quad (3)$$

This transformation can also be applied to any three-phase variables such as instantaneous current and stator flux linkages.

B. Park Transformation

Park transformation or *dq0* transformation converts three-phase stationary vector quantities into a rotating reference frame, also known as *dq*-frame. In other words, Park Transformation is a made up of Clarke Transformation that includes rotation angle, θ. This time-varying parameter simplifies complicated machine and power system problems [6]. Park transformation and its inverse transformation are represented by (4) and (5), where it is also applicable to any three-phase variables. v_d is the *d*-axis instantaneous voltage, whereas v_q is the *q*-axis instantaneous voltage on the *dq*-frame.

$$\begin{bmatrix} v_d \\ v_q \\ v_0 \end{bmatrix} = \sqrt{\frac{2}{3}} \begin{bmatrix} \cos(\theta) & \cos\left(\theta - \frac{2\pi}{3}\right) & \cos\left(\theta + \frac{2\pi}{3}\right) \\ -\sin(\theta) & -\sin\left(\theta - \frac{2\pi}{3}\right) & -\sin\left(\theta + \frac{2\pi}{3}\right) \\ \frac{1}{\sqrt{2}} & \frac{1}{\sqrt{2}} & \frac{1}{\sqrt{2}} \end{bmatrix} \begin{bmatrix} v_a \\ v_b \\ v_c \end{bmatrix} \quad (4)$$

$$\begin{bmatrix} v_a \\ v_b \\ v_c \end{bmatrix} = \sqrt{\frac{2}{3}} \begin{bmatrix} \cos(\theta) & -\sin(\theta) & \frac{1}{\sqrt{2}} \\ \cos\left(\theta - \frac{2\pi}{3}\right) & -\sin\left(\theta - \frac{2\pi}{3}\right) & \frac{1}{\sqrt{2}} \\ \cos\left(\theta + \frac{2\pi}{3}\right) & -\sin\left(\theta + \frac{2\pi}{3}\right) & \frac{1}{\sqrt{2}} \end{bmatrix} \begin{bmatrix} v_d \\ v_q \\ v_0 \end{bmatrix} \quad (5)$$

In a balanced condition, zero-sequence voltage can be eliminated and thus (4) can be expressed as (6):

$$\begin{bmatrix} v_d \\ v_q \end{bmatrix} = \sqrt{\frac{2}{3}} \begin{bmatrix} \cos(\theta) & \cos\left(\theta - \frac{2\pi}{3}\right) & \cos\left(\theta + \frac{2\pi}{3}\right) \\ -\sin(\theta) & -\sin\left(\theta - \frac{2\pi}{3}\right) & -\sin\left(\theta + \frac{2\pi}{3}\right) \end{bmatrix} \begin{bmatrix} v_a \\ v_b \\ v_c \end{bmatrix} \quad (6)$$

C. Phase-Locked Loop (PLL)

Phase-locked loop is a vital part of a grid-connected system as it is used to synchronize the phase angle and frequency [8] of the connected system with the grid in reference to the values at PCC. PLL is a negative-feedback system mainly consisting of a phase detector, a loop filter, and a voltage controlled oscillator (VCO). A phase detector is utilized to compare the input and VCO phase angles and generate the phase error to be filtered by the loop filter. Loop filter produces a control output that is sent to VCO in order to change its frequency in reference to the phase error [9]. Through negative-feedback process, the phase difference of utility voltage vector and a voltage reference frame input can be reduced. A block diagram of PLL used in a three-phase system is shown in Fig. 2.

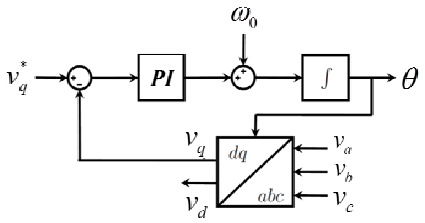

Fig. 2 Block diagram of PLL in three-phase system

From Fig. 2, the phase detector compares the voltage reference frame v_{q^*} and the vector of three-phase voltage, v_a, v_b, v_c transformed in the *dq*-form. Difference between v_q and v_{q^*} is sent to Proportional-Integral (PI) controller to produce angular speed values that will be compared with the actual angular speed, ω_0. The difference in angular speed will be integrated into a phase angle, θ, that is assigned to the VCO in order to change its frequency in a way that reduces the phase error. This process will eventually synchronize the three-phase voltage with the reference frame.

D. Current Control

Current control is a method to drive three-phase current flowing in AC loads to follow the reference signal values in an internal loop section of the control system [10]. A representative of current control block diagram is shown in Fig. 3. From Fig. 3, current reference values, i_d^{ref}, i_q^{ref} are used to be tracked by *dq*-frame instantaneous current, i_d and i_q transformed from three-phase current values supplied by the inverter. Difference between the current reference values and current sensor values are sent to the PI controller which will produce derivative and integral values of the error to be compared to the *dq*-voltage and voltage drop across inductor filter, *L*.

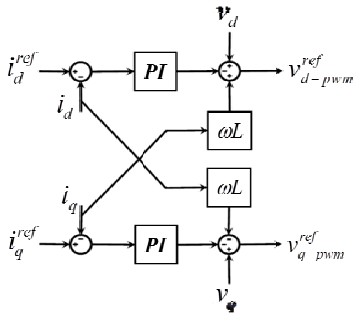

Fig. 3 Block diagram of current control method

E. Voltage Control

In a cascaded control system of grid-forming inverter, voltage control forms the external loop section, which is the outer loop of current control [11]. The voltage control block diagram is shown in Fig. 4. PI controllers are used to process the error between *dq*-frame reference voltage, v_d^{ref}, v_q^{ref} and actual voltage values, v_d , v_q, making the output value closer to the reference value and generating current reference values for current control.

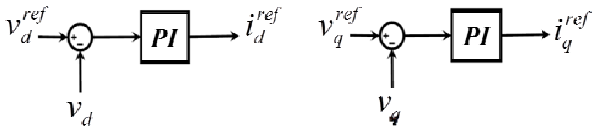

(a) v_d control (b) v_q control

Fig. 4 Block diagram of voltage control

IV. Grid-Injecting Mode Control

A. Active and Reactive Power Control

In grid-injecting mode, power control performs the similar function as voltage control in grid-forming mode, in which it defines the error between reference and actual power values and producing its corresponding current reference values for current control.

B. Droop Control

Droop power control is a method to maintain the grid voltage amplitude and frequency under control limitations by balancing the active and reactive power transfer to and from the common AC bus [11]. Increment or decrement in loading will result in a change of active power demand that is closely related to frequency change. Increase in active power demand will induce frequency reduction of a generating unit, and therefore load-frequency control (LFC) of multiple generating units is vital to maintain a balanced power alternation [6]. Thus, each generating unit has a particular droop characteristic, which is represented by the gradient of the graph, k_p, as shown in Fig. 5 (a). f_0, f are the rated and actual frequency, V_0, V are the rated and actual voltage, P_0, P are the rated and actual active power, whereas Q_0 , Q are the rated and actual reactive power respectively.

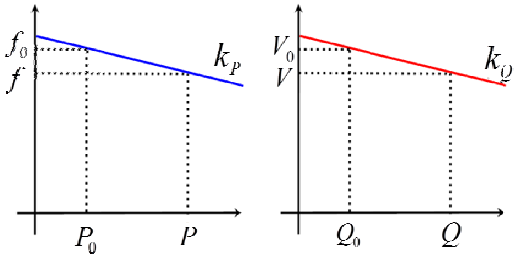

(a) Frequency-Active Power (b) Voltage-Reactive Power

Fig. 5 Droop control characteristics

Droop characteristic is usually represented in percentage (%) droop. For a particular droop characteristic, for instance 10% droop, 10% change in frequency will result in 100% change in active power output. In other words, the lower the droop characteristic value, the higher the stability limit of the whole system [12]. This also applies to voltage magnitude change that will affect reactive power values. Droop control based on active and reactive power and its correlation with voltage and frequency is explained in (7)~(16).

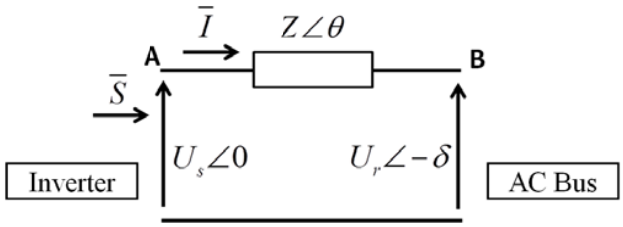

Fig. 6 Power flow from inverter to common AC bus

From Fig. 6, $U_s\angle 0$ is the voltage at sending side, or the open voltage of the inverter, $U_r\angle -\delta$ is the voltage at receiving side, or the common AC bus voltage, $\bar{I}$ is the current from inverter, and $Z\angle\theta$ is the impedance between inverter and common AC bus [13]. The apparent power flow from point A to point B is

$$\bar{S} = \overline{U_s}\bar{I}^* = \overline{U_s}\left(\frac{\overline{U_s}-\overline{U_r}}{\bar{Z}}\right)^* \quad (7)$$

and by including the phase difference, the apparent power, $\bar{S}$ can also be expressed as (8) and the corresponding active power, P and reactive power, Q are defined in (9) and (10) [14].

$$\bar{S} = \left(\frac{U_s^2}{Z}e^{j\theta} - \frac{U_sU_r}{Z}e^{j(\delta+\theta)}\right) \quad (8)$$

$$P = \frac{U_s^2}{Z}\cos\theta - \frac{U_sU_r}{Z}\cos(\delta+\theta) \quad (9)$$

$$Q = \frac{U_s^2}{Z}\sin\theta - \frac{U_sU_r}{Z}\sin(\delta+\theta) \quad (10)$$

$Ze^{j\theta} = R + jX$ is inserted in (9), (10) to form (13), (14) that was simplified to show relation of the equations with voltage and frequency respectively.

$$\frac{RP+XQ}{U_s} = U_s - U_r\cos\delta \quad (11)$$

$$\frac{XP-RQ}{U_s} = U_r\sin\delta \quad (12)$$

The power angle δ is approximated to zero for a small change, and in most cases reactance, X is much bigger than resistance, R. Thus,

$$\frac{XQ}{U_s} = U_s - U_r \quad (13)$$

$$\frac{XP}{U_s} = \delta \quad (14)$$

where power angle is controlled by frequency as stated in [14]. From (13) and (14), it is clear that reactive power is directly proportional to voltage difference, and active power is directly proportional to frequency. Therefore, active and reactive power can be controlled directly by adjusting frequency and voltage values respectively. This can be represented in the following equations.

$$f - f_0 = -k_p(P - P_0) \quad (15)$$
$$V - V_0 = -k_q(Q - Q_0) \quad (16)$$

$f - f_0$ is the difference between actual and rated frequency, whereas $V - V_0$ is the difference between actual and rated voltage. k_p and k_q are the droop characteristics for active power and reactive power respectively. This relationship can be clearly seen in Fig. 5. These equations were used in implementing droop power control in grid-injecting mode of inverter, and in this study, only frequency droop was implemented as the grid-connected inverter was operated under unity power factor.

V. Experimental Methodology

A. Grid-forming Inverter Control

In stand-alone mode, power control and current control was installed in the grid-connected inverter, but PLL was not necessary, as the inverter output need not to be synchronized with the grid. The control block diagram used in this mode is shown in Fig. 7 and the experimental circuit used in this mode is shown in Fig. 8. The parameters used in this mode of experiment are shown in Table I. Control block diagram in Fig. 7 is the exact representative of the control scheme explained in the previous section.

In this scheme, the power control loop will provide reference values for the internal current control loop and four PI controllers were used simultaneously, which are P, Q, i_d, and i_q controllers. In this experiment, reactive power, Q, was set to zero to provide a unity power factor condition whereas active power, P, was the controlled variable. The inverter was operated under PWM voltage reference command provided by current control block for switching process in the inverter circuit.

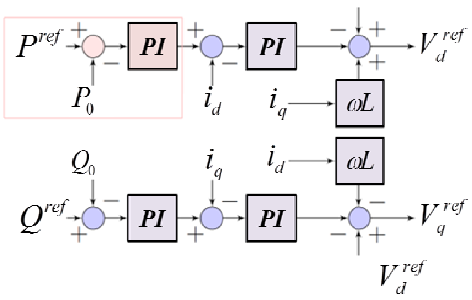

Fig. 7 Control scheme block diagram

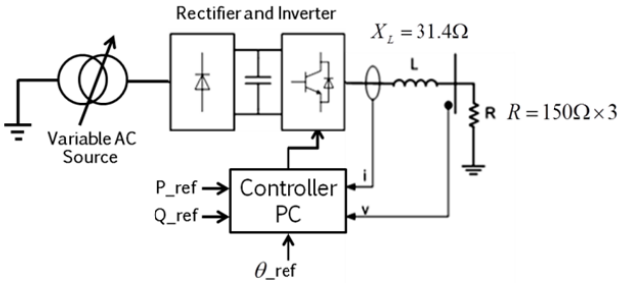

Fig. 8 Grid-forming mode experimental circuit

TABLE I
GRID-FORMING MODE EXPERIMENTAL PARAMETERS

Symbol	Quantity	Value
V_{in}	AC input voltage	150 V
L	Inductance	100 mH
R	Resistance	42 Ω

According to Fig. 8, the output of the inverter was filtered using inductance to filter out harmonic components. P_ref and Q_ref are the reference values for active power and reactive power respectively, where Q_ref is set to be zero. θ_ref is the phase angle reference value which was generated from the controller internally. The control scheme was compiled using C-language codes and transformed into binary file to be downloaded into the Digital Signal Processor (DSP) chip in the control board of the inverter.

B. Grid-Injecting Inverter Control

Prior to synchronization to the grid, voltage control is required in order to ensure the same voltage levels at the inverter side and PCC. Voltage reference values were obtained from the PCC that represent the grid voltage parameters. After achieving the same voltage and frequency levels, synchronization was executed by turning on the synchroscope switch as shown in Fig. 9. During the synchronization process, power control was performed to operate the grid-connected inverter.

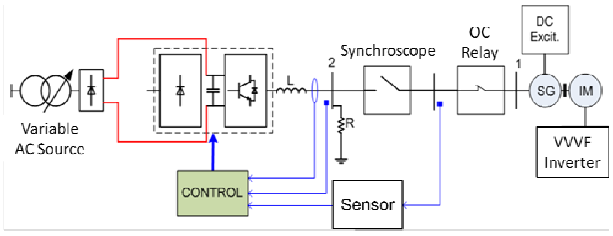

Fig. 9 Grid-injecting mode experimental circuit

Hence, grid-forming mode control has two external loops consisting of voltage control and power control. Each of these control blocks will provide current reference values for current control to provide switching information for the inverter through PWM. The parameters used in this mode of experiment are shown in Table II. Different from grid forming experiment, a synchronous generator was used as the generating unit at the grid side as it can easily change its frequency by adjusting the rotor speed.

TABLE II
GRID-INJECTING MODE EXPERIMENTAL PARAMETERS

Symbol	Quantity	Value
V_{DC}	DC input voltage	337V
L	Inductance	33mH
R	Resistance	125Ω

Next to the synchronous generator, an over current relay (OC Relay) was connected to prevent abnormal current values from flowing in the circuit. In the control codes of this experiment, two PLL blocks were required. At the inverter side, PLL was required to control the power, voltage and current through *dq*-transformation. At the grid side, PLL input acquired from the PCC that includes grid phase angle, frequency, and voltage levels were used as the reference for the voltage control in order to prepare for synchronization process, or known as the pre-synchronization process.

VI. RESULTS AND DISCUSSION

A. Grid-Forming Mode Experiment

In this experiment, reactive power reference value was set to zero, whereas active power reference value was changed from 20 W to 120 W. The actual active power value followed the change in active power reference value as shown in Fig. 10. The active power reference value was compared with the actual active power value at that time to calculate the error. The error was then fed into PI controller in order to generate the corrected value to be assigned to the inverter. After the reference value change was done, the inverter generated an output that followed the exact value as the reference value.

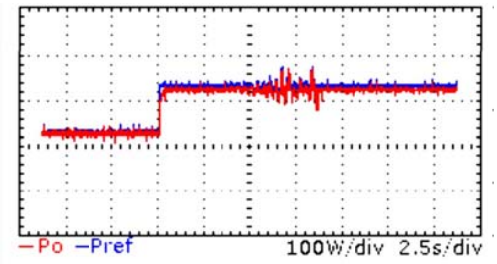

Fig. 10 Grid-forming mode active power control experiment result

B. Grid-Injecting Droop Power Control

In this experiment, droop characteristic was first assigned to the inverter and the output from the inverter generated a power output that was based on the droop gradient and the frequency of the system. In a dispersed generation system, each of different generating units has a droop characteristic that allows a simultaneous power generation and load sharing, but in this experiment, different droop characteristics were only assigned to the inverter. In this study, three droop characteristics, 40%, 50% and 60%, were used. The balance of power and frequency of this system depends on the power generated by droop power control of the grid-connected inverter. The experimental result is shown in Fig. 11. From Fig. 11, the result obtained was compared with the theoretical value calculated by using (17),

$$P_{ref} = P_{base} - \frac{1}{k_{droop}}(f_{PCC} - f_{base}) \quad (17)$$

where P_{ref} is the active power reference value, P_{base} is the base active power, k_{droop} is the droop gradient or the droop characteristic, f_{PCC} is the frequency at the point of common coupling, and f_{base} is the base frequency.

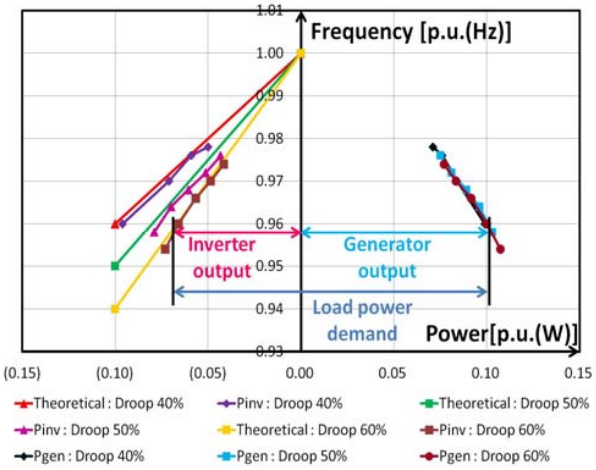

Fig. 11 Droop control theoretical and experimental result

The base frequency and the base power of this system were 50Hz and 1kW respectively. Droop power control in this experiment was created to be operating in a limited range between 50W (0.05p.u.) and 150W (0.15p.u.) that was already assigned in the programming code. In order to imitate the increment and decrement in load power demand, a three-phase variable resistor was used. Increment in load power demand will cause a small frequency drop that will induce increment in power output from the generating units. From Fig. 11, during load demand increment at 40% droop, the inverter increased its power output and took more power supplying proportion compared to the synchronous generator. The synchronous generator generated an output that followed the remaining power required according to the output from the inverter. During 60% droop, the inverter generated a lesser power output change compared to the synchronous generator as the droop characteristic of the inverter has a higher gradient value.

VII. Conclusion

From the results obtained, output power level at the microgrid side will follow the power level change at the grid side during droop control in accordance to the increment and decrement of the load capacity. The frequencies at both sides were maintained within a nominal range. Hence, small-scale microgrid system was established using experimental modules that represent vital parts of the system including inverter, and a stabilized droop control was produced in this research. This laboratory scale microgrid system is expected to be a simulation model in learning environments and to analyze the problems that may happen in a real large-scale microgrid system.

References

[1] F. Blaabjerg, R. Teodorescu, M. Liserre, A.V. Timbus, "Overview of Control and Grid Synchronization for Distributed Power Generation Systems," *IEEE Trans. Ind. Electron.*, vol. 53, no. 5, pp. 1398–1409, Oct. 2006.

[2] B. Kroposki *et al.*, "Making Microgrids Work," *IEEE Power & Energy Magazine*, May/June 2008, pp. 40–53.

[3] R. Lasseter *et al.*, "Integration of Distributed Energy Resources: The CERTS MicroGrid Concept," Lawrence Berkeley National Laboratory, prepared for Transmission Reliability Program and Energy Systems Integration Program, Apr. 2010, pp. 6–19.

[4] N. Hatziargyriou, H. Asano, R. Iravani, C. Marnay, "Microgrids: An Overview of Ongoing Research, Development, and Demonstration Projects," *IEEE Power & Energy Magazine*, July/August 2007, pp. 78–94.

[5] J. C. Vasquez, J. M. Guerrero, A. Luna, P. Rodríguez, R. Teodorescu, "Adaptive Droop Control Applied to Voltage-Source Inverters Operating in Grid-Connected and Islanded Modes," *IEEE Trans. Ind. Electron.*, vol. 56, no. 10, pp. 4088–4096, Oct. 2009.

[6] Prabha Kundur, *Power System Stability and Control.* U.S.A.: McGraw-Hill Inc., 1994, pp. 67–582.

[7] H. Akagi, E. H. Watanabe, M. Aredes, *Instantaneous Power Theory and Applications to Power Conditioning*. New Jersey: John Wiley and Sons, Inc., 2007, pp. 43–47.

[8] G. C. Hsieh, J. C. Hung, "Phase-Locked Loop Techniques-A Survey," *IEEE Trans. Ind. Electron.*, vol. 43, no. 6, pp. 609-615, Dec. 1996.

[9] F. M. Gardner, *Phaselock Techniques.* New Jersey: John Wiley & Sons, Inc., 2005, pp. 1–3.

[10] M. P. Kazmierkowski, L. Malesani, "Current Control Techniques for Three-Phase Voltage-Source PWM Converters," *IEEE Trans. Ind. Electron.*, vol. 45, no. 5, pp. 691–703, Oct. 1998.

[11] J. Rocabert, A. Luna, F. Blaabjerg, P. Rodriguez, "Control of Power Converters in AC Microgrids," *IEEE Trans. Power Electronics*, vol. 27, no. 11, pp. 4734–4749, Nov. 2012.

[12] P. Arboleya *et al.*, "An improved control scheme based in droop characteristic for microgrid converters," *Electric Power Systems Research 80*, pp. 1215–1221, June 2010.

[13] J. Matas, M. Castilla, L. G. Vicu˜na, J. Miret, "Virtual Impedance Loop for Droop-Controlled Single-Phase Parallel Inverters Using a Second-Order General-Integrator Scheme," *IEEE Trans. Power Electronics*, vol. 25, no. 12, pp. 2993–3002, Dec. 2010.

[14] K. D. Brabandere, B. Bolsens, J. V. Keybus, A. Woyte, "A Voltage and Frequency Droop Control Method for Parallel Inverters," *IEEE Trans. Power Electronics*, vol. 22, no. 4, pp. 1107–1115, July 2007.

N. A. Jalalludin was born in Pahang, Malaysia on the 25th of July 1990. She received the B.E. in electrical engineering from Department of Electrical Engineering, Tokyo University of Science, Japan, in 2013 and she is currently pursuing M.E. degree at Power System Laboratory in the field of electrical engineering at Shibaura Institute of Technology, Japan. Her research interests include hydrogen storage system, power electronics and inverter topologies.

A. Rizqiawan received the B.E. and M.E. degrees in electrical engineering from the School of Electrical Engineering and Informatics, Institute of Technology Bandung, Indonesia, in 2006 and 2008, respectively. He pursued the Ph.D. degree at Power System Laboratory, Shibaura Institute of Technology, Japan. He is currently a research assistant on School of Electrical Engineering and Informatics, Institute of Technology Bandung, Indonesia. His research interests include distributed generation and application of power electronics in power system.

Prof. G. Fujita received the B.E., M.E., and Ph.D. degrees in electrical engineering from Hosei University, Japan in 1992, 1994 and 1997 respectively. In 1997, he was a research student at Tokyo Metropolitan University, Japan. He is currently a Professor in Shibaura Institute of Technology, Japan. He is a member of IEEE and also a First Class Licensed Engineer of Electric Facility in Japan. His research interests include power system control including dispersed power systems.